

# *Streptomyces zerumbet*, a Novel Species from *Zingiber zerumbet* (L.) Smith and Isolation of Its Bioactive Compounds

Thongchai Taechowisan<sup>1\*</sup>, Winyou Puckdee<sup>1</sup>, Waya S. Phutdhawong<sup>2</sup>

<sup>1</sup>Department of Microbiology, Faculty of Science, Silpakorn University, Nakorn Pathom, Thailand

<sup>2</sup>Department of Chemistry, Faculty of Science, Silpakorn University, Nakorn Pathom, Thailand

Email: \*tewson84@hotmail.com

**How to cite this paper:** Taechowisan, T., Puckdee, W. and Phutdhawong, W.S. (2019) *Streptomyces zerumbet*, a Novel Species from *Zingiber zerumbet* (L.) Smith and Isolation of Its Bioactive Compounds. *Advances in Microbiology*, 9, 194-219. <https://doi.org/10.4236/aim.2019.93015>

**Received:** February 18, 2019

**Accepted:** March 12, 2019

**Published:** March 15, 2019

Copyright © 2019 by author(s) and Scientific Research Publishing Inc. This work is licensed under the Creative Commons Attribution International License (CC BY 4.0).

<http://creativecommons.org/licenses/by/4.0/>



Open Access

## Abstract

*Streptomyces zerumbet* W14, a novel species of the endophyte genus *Streptomyces* was isolated from the rhizome tissue of *Zingiber zerumbet* (L.) Smith. Identification of strain W14 was based on its morphology, chemotaxonomy and phylogenetic analysis using 16S rDNA sequence. It was classified as the secondary metabolites of the culture extract were studied. The major active ingredients from the crude extract were purified by silica gel column chromatography and identified by spectroscopic data. The crude extract and purified compounds were tested for their biological activities on antibacterial and anti-inflammatory properties. The crude extract showed inhibition on the growth of Gram-positive bacteria with the MIC and MBC values of 8 - 32 µg/ml and 32 - 128 µg/ml, respectively. The isolated compounds were identified to be methyl 5-(hydroxymethyl)furan-2-carboxylate (**1**) and geldanamycin (**2**). Bioassay studies showed that compound **1** had antibacterial activity against *Staphylococcus aureus* ATCC 25923 and Methicillin Resistant *S. aureus* strain Sp6 (clinical isolate) with the MIC and MBC values of 1 µg/ml and 16 - 64 µg/ml, respectively, and also showed activity against Bacillus Calmette-Guérin (vaccine strain) with MIC and MBC values of 128.00 µg/ml and 128.00 µg/ml, respectively. The compound **2** at the concentration of 1 - 5 µg/ml had *in vitro* anti-inflammatory activity on LPS-induced RAW 264.7 cells by inhibition of mRNA expression and production of inducible NO synthase (iNOS), tumor necrosis factor- $\alpha$  (TNF- $\alpha$ ), interleukin-1 $\beta$  (IL-1 $\beta$ ), and interleukin-6 (IL-6). These results suggest that compounds **1** and **2** produced by *S. zerumbet* W14 (an endophyte of *Z. Zerumbet*) have antibacterial and anti-inflammatory activities, respectively. Therefore, the future studies on these compounds could be useful for the management of bacterial infections and inflammatory diseases.

---

## Keywords

Antibacterial Activity, Anti-Inflammatory Activity, Endophytic Actinomycetes, Geldanamycin, Methyl 5-(Hydroxymethyl)Furan-2-Carboxylate, *Zingiber zerumbet*

---

## 1. Introduction

Inside the tissue of nearly all the healthy plants, there are many endophytic microorganisms. Endophytes are synergistic to their host, some of them produced secondary metabolites which exhibit plant growth promoters or prevent phytopathogen attacking. During our investigations of the endophytes, we isolated an endophytic actinomycete from the root tissues of *Zingiber officinale* Rosc. and it was identified as *Streptomyces aureofaciens* CMUAc130; it showed the most effective antifungal activity [1]. The major active ingredients from the culture filtrate were identified as 5,7-dimethoxy-4-*p*-methoxyphenylcoumarin and 5,7-dimethoxy-4-phenylcoumarin which have antifungal activity [2]. We report here the isolation from the rhizome of *Zingiber zerumbet* (L.) Smith of another *Streptomyces zerumbet* W14, a novel species which was identified by morphology, chemotaxonomy and phylogenetic analysis. Extraction of the culture medium this strain afforded methyl 5-(hydroxymethyl)furan-2-carboxylate (1) and geldanamycin (2), which displayed very strong antibacterial and anti-inflammatory activities, respectively.

## 2. Materials and Methods

### 2.1. Cultivation, Determination, Extraction and Isolation

Leaf, stem, rhizome and root tissues of *Zingiber zerumbet* (L.) Smith were used to isolate the endophytic actinomycetes by surface-sterilization technique and validation of surface sterilization was performed as described in our previous studies [3] [4]. Strain W14 was selected and identified using morphological, cultural, physiological and biochemical characteristics, chemotaxonomy and 16S rDNA sequencing [1]. This strain was grown on ISP-2 agar at 30°C for 14 days and then the culture medium was cut into small pieces that were extracted with ethyl acetate (3 × 500 ml). This organic solvent was pooled and then taken to dryness under rotary evaporation to give a dark brown solid. The solid was separated by column chromatography using silica gel 60 (Merck, 0.040 - 0.063 mm) and 30%, 50%, 75% and 100% of ethyl acetate in hexane as the eluent to give 17 main fractions (F1-F17). Fraction F17 (8.0 mg) gave a very prominent single spot of pure compound 1 on TLC and was undertaken to investigate on NMR spectroscopy. Fractions 9 - 13 was pooled and fractionated again by column chromatography using sephadex LH-20 (Sigma) and 50% of methanol in dichloromethane as the eluent to give 31 fractions. Fraction F13 (30.3 mg) gave a very prominent single spot of pure compound 2 on TLC and was undertaken to

investigate on NMR spectroscopy.

## 2.2. Antimicrobial Activity Assay

An *in vitro* plate technique was used to test the inhibitory effects of strain W14 on the tested bacteria. For screening of antibacterial activity, crude extract and purified compounds were tested against *S. aureus* ATCC 25932, *B. cereus* ATCC 7064, *B. subtilis* ATCC 6633, *Escherichia coli* ATCC 10536, *Salmonella* Typhi ATCC 19430, *Pseudomonas aeruginosa* ATCC 27853, *Serratia marcescens* ATCC 8100, Methicillin Resistant *S. aureus* strain Sp6 (clinical isolate) and Bacillus Calmette-Guérin (vaccine strain) using the paper disk method of National Committee for Clinical Laboratory Standards [5]. Ampicillin (30 unit/disk) and chloramphenicol (30 µg per disk) (Oxoid, UK) were used as references for antimicrobial activity, as described in our previous study [4]. For bioautography assay, the crude extract and purified compounds were separated by TLC in optimum solvent system. The TLC strips were sterilized by exposing to UV for 30 min. Tested bacteria were grown on nutrient broth at 37°C for 24 h. The bacteria cells were diluted to be 10<sup>5</sup> cells/ml in melted soft agar and then were overlaid on TLC strips placed on ISP-2 plates. The plates were incubated at 37°C for 24 h, then the inhibition zone was observed.

## 2.3. Minimum Inhibitory Concentrations

The MICs of the crude extract and purified compounds were determined by NCCLS microbroth dilution methods [6]. Ampicillin and chloramphenicol were used as references for antibacterial activity. The test samples were first of all dissolved in DMSO. The range of sample dilutions was 512 - 0.5 µg/ml in nutrient broth supplemented with 10% glucose and 0.05% phenol red (NBGP). 100 µl of each concentration was added in each well (96-wells microplate) containing 95 µl of NBGP and 5 µl of inoculum (standardised at 1.5 × 10<sup>6</sup> CFU/ml by adjusting the optical density to 0.1 at 600 nm SHIMADZU UV-120-01 spectrophotometer). The final concentration of DMSO in the well was less than 1% (preliminary analyses with 1% (v/v) DMSO/NBGP affected neither the growth of the test organisms nor the change of colour due to this growth). The negative control well consisted of 195 µl of NBGP and 5 µl of the standard inoculum. The plates were covered with a sterile plate sealer, then agitated to mix the content of the wells using a plate shaker and incubated at 37°C for 24 h. The assay was repeated twice. Microbial growth was determined by observing the change of colour in the wells (red when there is no growth and yellow when there is growth). The lowest concentration showing no colour change was considered as the MIC. For the determination of Minimum bactericidal concentration (MBC), a portion of liquid (10 µl) from each well that showed no change in colour was plated on nutrient agar and incubated at 37°C for 24 h. The lowest concentration that yielded no growth after this sub-culturing was taken as the MBC.

## 2.4. Cell Culture and Sample Treatment

HeLa cell line, L929 murine fibroblast cell line, and RAW 264.7 murine macrophage cell line was obtained from the Korean Cell Line Bank (Seoul, Korea). Human peripheral blood mononuclear cells (PBMCs) were isolated by density centrifugation with Ficoll-Paque [7]. These cells were grown at 37°C in DMEM medium supplement with 10% FBS, penicillin (100 units/ml), and streptomycin sulfate (100 µg/ml) in a humidified atmosphere of 5% CO<sub>2</sub>.

## 2.5. MTT Assay for Cell Viability

Cytotoxicity studies were performed on a 96-well plate. The cells were mechanically scraped and plated  $2 \times 10^5$  per well containing 100 µl of DMEM medium with 10% FBS and incubated overnight. The crude extract and purified compounds **1** and **2** were dissolved in dimethylsulfoxide (DMSO) for stock solution. Cells were incubated with crude extract and purified compounds **1** and **2** at increasing concentrations and stimulated with LPS 1 µg/ml for 24 h. The DMSO concentrations in all assays did not exceed 0.1%. Twenty-four h after seeding, 100 µl new media or test compound was added, and the plates were incubated for 24 h. Cells were washed once before adding 50 µl FBS-free medium containing 5 mg/ml MTT. After 4 h of inoculation at 37°C, the medium was discarded and the formazan blue, which formed in the cells, was dissolved in 50 µl DMSO. The optical density was measured at 450 nm. The concentration required for reducing the absorbance by 50% (IC<sub>50</sub>) compared to the control cells was determined.

## 2.6. Nitrite Assay

Nitrite accumulation, an indicator of NO synthesis, was measured in the culture medium by Griess reaction [8]. Briefly, 100 µl of cell culture medium was mixed with 100 µl of Griess reagent [equal volumes of 1% (w/v) sulfanilamide in 5% (v/v) phosphoric acid and 0.1% (w/v) naphthylethylenediamine-HCl] and incubated at room temperature for 100 min] and then the absorbance at 550 nm was measured in a microplate reader. Fresh culture medium was used as the blank in all experiments. The amount of nitrite in the samples was calculated from a sodium nitrite standard curve freshly prepared in culture medium.

## 2.7. PGE<sub>2</sub>, TNF-α, IL-1β and IL-6 Assay

PGE<sub>2</sub>, TNF-α, IL-1β and IL-6 level in macrophage culture medium were quantified by ELISA kits (eBioscience, CA, USA) according to the manufacturer's instructions.

## 2.8. Western Blot Assay

Cellular proteins were extracted from control and test compound-treated RAW 264.7 cells as described in our previous study [9]. Protein concentration was determined by BioRad protein assay reagent according to the manufacturer's instructions, 40 - 50 µg of cellular proteins from treated and untreated cell extracts were electroblotted onto nitrocellulose membrane followed by separation on

10% SDS-polyacrylamide gel electrophoresis. The immunoblot was incubated overnight with blocking solution (5% skim milk) at 4°C, followed by incubation for 4 h with a 1:500 dilution of monoclonal anti-iNOS or COX-2 antibody (Santacruz, CA, USA). Blots were washed 2 times with PBS and incubated with a 1:1000 dilution of horseradish peroxidase-conjugated goat anti-mouse IgG secondary antibody (Santacruz, CA, USA) for 1 h at room temperature. Blots were again washed three times in Tween 20-Tris-buffered saline and then developed with the colorimetric substrate 3,3',5,5'-tetramethylbenzidine (SurModics, MN, USA). The signals were quantified using gel image-analysis software V1.7.8 (GelQuant.NET, BiochemLabSolutions.com, USA).

### **2.9. Inhibition of Pro-Inflammatory Mediator and Cytokine Gene Expressions**

The expression of pro-inflammatory mediator and cytokine genes was investigated by reverse transcription—polymerase chain reaction (RT-PCR). RAW 264.7 cells were incubated with compounds **1** and **2** at different concentrations (1, 2.5, 5 and 10 µg/ml) and stimulated with LPS 1 µg/ml at 37°C in FBS-free medium for 24 h. RAW 264.7 cells at for 24 h. Total RNA was extracted from RAW 264.7 cells after treatment with purified compounds, The cells were lysed with Trizol<sup>®</sup> and centrifuged at 12,000 rpm for 15 min at 25°C, following the addition of chloroform. Isopropanol was added to the supernatant at a 1:1 ratio and the RNA pellet was obtained following centrifugation. After washing with ethanol, extracted RNA was solubilized in diethyl pyrocarbonate-treated RNase-free water and quantified by measuring the absorbance at 260 nm. Equal amounts of RNA (1 µg) were reverse transcribed in a master mix containing 1X reverse transcriptase (RT) buffer, 1 mM dNTPs, 500 ng of oligo(dT)<sub>15</sub> primers, 140 U of murine Moloney leukaemia virus reverse transcriptase and 40 U of RNase inhibitor, for 45 min at 42°C. PCR was carried out in an automatic thermal cycler (Perkin-Elmer Cetus) to amplify iNOS, TNF- $\alpha$ , IL-1 $\beta$ , IL-6 and  $\beta$ -actin mRNA. Primer sequences used to amplify the desired cDNA were shown in **Table 1**. The PCR products electrophoresed on 2% agarose gels and were visualized by ethidium bromide staining and quantified using gel image-analysis software V1.7.8 (GelQuant.NET, BiochemLabSolutions.com, USA).

### **2.10. Data Analysis**

Data are reported as mean  $\pm$  SEM values of three independent determinations. Statistical analysis was performed by Student's *t*-test.

## **3. Results**

### **3.1. Identification and Description of Selected Actinomycete Isolate**

Eighteen actinomycete isolates were obtained, 4 of which were isolated from leaves, 5 isolates from rhizomes, 8 isolates from roots and only one isolate from

**Table 1.** Primers used in reverse transcription-polymerase chain reaction analysis.

Gene <sup>a</sup>	Primer sequences (5' - >3')	PCR product size (bp)
iNOS	5'-CCCTTCCGAAGTTTCTGGCAGCAGC-3' (sense) 5'-GGCTGTCAGAGCCTCGTGGCTTTGG-3' (antisense)	496
TNF- $\alpha$	5'-TTGACCTCAGCGCTGAGTTG-3' (sense) 5'-CCTGTAGCCCCACGTCGTAGC-3' (antisense)	364
IL-1 $\beta$	5'-CAGGATGAGGACATGAGCACC-3' (sense) 5'-CTCTGCAGACTCAAACCTCCAC-3' (antisense)	447
IL-6	5'-GTACTCCAGAAGACCAGAGG-3' (sense) 5'-TGCTGGTGACAACCACGGCC-3' (antisense)	308
$\beta$ -actin	5'-GTGGGCCGCCCTAGGCACCAG-3' (sense) 5'-GGAGGAAGAGGATGCGGCAGT-3' (antisense)	603

<sup>a</sup>iNOS, Inducible nitric oxide synthase; TNF- $\alpha$ , Tumor necrosis factor- $\alpha$ ; IL-1 $\beta$ , Interleukin-1 $\beta$ ; IL-6, Interleukin-6.

stems. The strain W14 showed promising activities against *S. aureus* ATCC 25932, *B. cereus* ATCC 7064 and *B. subtilis* ATCC 6633. However the other isolates had no potential of antibacterial activity to the tested bacteria. Therefore, all subsequent experiments involved the use of the strain W14. Based on results in the presence of LL-type diaminopimelic acid in the whole-cell extracts, the strain W14 was identified as belonging to the genus *Streptomyces*. Direct sequencing of the PCR-amplified 16S rDNA of the strain W14 was determined from position 8 to position 1464 of the 16S rDNA gene sequence of *E. coli* numbering system [10]. This sequence corresponded to an estimated 95.7% of the total 16SrDNA primary sequence. BLAST search results for strain W14 came from non-redundant GenBank + EMBL + DDBJ; when reference sequences were chosen, unidentified and unpublished sequences were excluded. The BLAST search results and the phylogenetic tree (Figure 1) generated from representative strains of the related genera showed that strain W14 had high levels of sequence similarity to species of *S. malaysiensis* (accession number: AB249918). 16S rDNA analysis revealed that strain W14 is phylogenetically closely related to *S. malaysiensis* (the sequence similarity levels were 99.65%). The nucleotide sequence data reported in this paper appeared in the Gen-Bank, EMBL and DDBJ databases with the accession number AB845431. As well as in morphological observation of the 2 - 3 weeks old culture of the strain W14 grown on yeast extract-malt extract agar (ISP-2) revealed that both the aerial and vegetative hyphae were abundant, well developed and not fragmented. Mature spore chains were extended spirals with rugose-surfaces (Figure 2). The strain W14 had an aerial mass color in the white-grey series on ISP-2. The substrate mycelium of W14 showed light grayish olive to moderate olive brown color. It also produced soluble deep yellow to dark yellow soluble pigments on ISP-2, Tyrosine agar (ISP-7) and Bennett's agar. It showed antimicrobial activity against *B. subtilis*, *S. aureus*, *Candida albicans*, *Aspergillus flavus* and *Aspergillus fumigatus*, but no activity against *E. coli* and *Aspergillus niger*. Strain W14 showed 3% - 5% tolerance

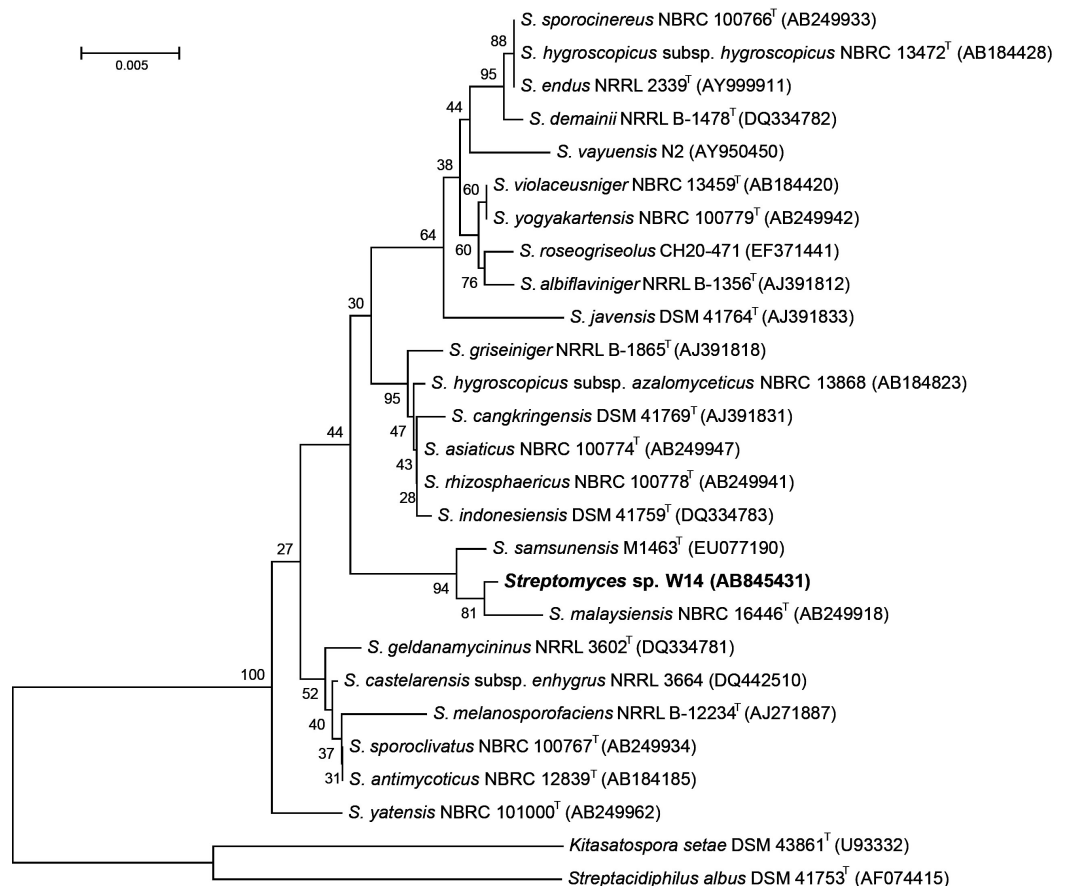


**Figure 1.** Neighbour-joining phylogenetic tree of the strain W14, including representatives of the most closely related type strains which were retrieved from GenBank, and accession numbers appear in parentheses. Bootstrap (1000 replicates) values are given in percentage. Bar, 0.005 substitutions per nucleotide.

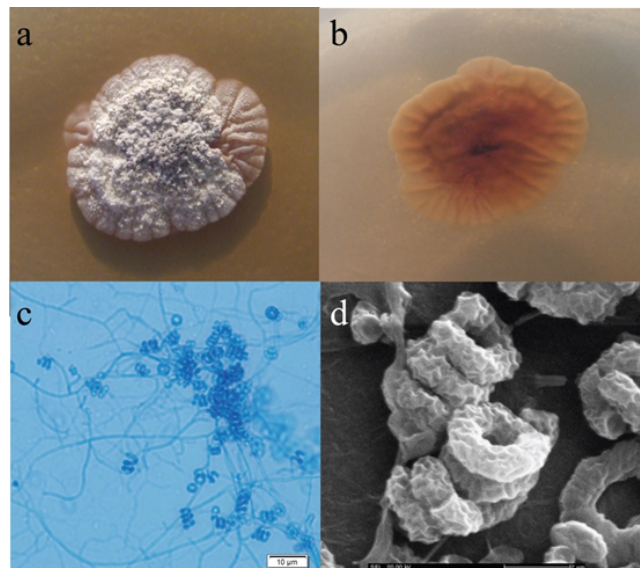


**Figure 2.** Morphological characteristics of the strain W14. The colony appearance ((a), surface; (b), reverse) on yeast extract-malt extract (ISP-2) agar plates after 2 weeks of incubation at 30°C. (c), light micrograph; Bar = 10 µm, and (d), scanning electron micrograph on ISP-2 agar (21 days); Bar = 2 µm.

to salt and grew well at pH 5.6 to 11.0, at 37°C but was unable to grown on temperature above 45°C. This strain utilized glucose, mannose, meso-inositol, sucrose, galactose, fructose, lactose, maltose, mannitol, mannose, raffinose, arabinose, sodium acetate and sodium citrate, but did not utilize xylose, sorbitol and CM-cellulose. It showed moderate activities of catalase, gelatinase and caseinase, hydrolysed casein, starch and tyrosine, but did not produce hydrogen sulphide. However, it also resisted ampicillin and erythromycin. A comparative analysis of the cultural and biochemical characteristics of strain W14 with respect to its phylogenetic relatives was shown in **Table 2** and **Table 3**.

**Table 2.** Phenotypic characteristics of strain W14 and related species of the genus *Streptomyces*. Strains: W14, *S. malaysiensis* DSM 41697<sup>T</sup> and *S. samsunensis* M1463<sup>T</sup>.

Characteristics	W14	DSM 41697 <sup>T</sup>	M1463 <sup>T</sup>
Antimicrobial activity against:			
<i>Bacillus subtilis</i>	+	+	+
<i>Escherichia coli</i>	-	-	-
<i>Staphylococcus aureus</i>	+	-	+
<i>Candida albicans</i>	+	+	+
<i>Aspergillus flavus</i>	+	No data	-
<i>Aspergillus fumigatus</i>	+	No data	No data
<i>Aspergillus niger</i>	-	No data	+
Decomposition of:			
Casein	+	+	+
Starch	+	+	+
L-Tyrosine	+	+	-
Xanthine	Not done	-	-
Growth at:			
4°C	-	-	-
37°C	+	+	+
45°C	-	-	-
pH 4.0	-	-	-
pH 5.6	+	+	+
pH 11.0	+	-	No data
Growth in the presence of:			
Lysozyme (0.005%, w/v)	+	+	No data
Sodium chloride (3%, w/v)	+	+	No data
Sodium chloride (5%, w/v)	+	-	No data
Resistance to antibiotics (ug):			
Ampicillin (10)	+	+	No data
Chloramphenicol (30)	-(16.9) <sup>a</sup>	-(15) <sup>a</sup>	+
Erythromycin (15)	+	-(18) <sup>a</sup>	No data



## Continued

Gentamicin sulphate (10)	-(45.6) <sup>a</sup>	-(28) <sup>a</sup>	-
Kanamycin sulphate (30)	-(33.0) <sup>a</sup>	-(34) <sup>a</sup>	No data
Neomycin sulphate (30)	-(35.6) <sup>a</sup>	-(30) <sup>a</sup>	-
Novobiocin sulphate (30)	Notdone	-(40) <sup>a</sup>	No data
Streptomycin sulphate (10)	-(18.0) <sup>a</sup>	-(35) <sup>a</sup>	-
Tetracycline hydrochloride (30)	-(36.3) <sup>a</sup>	-(20) <sup>a</sup>	No data
Ampicillin (10)	+	+	No data
Chloramphenicol (30)	-(16.9) <sup>a</sup>	-(15) <sup>a</sup>	+
Growth on sole carbon sources (1%, w/v)			
L-Arabinose	+	+	+
D-Fructose	+	+	+
D-Galactose	+	+	+
D-Glucose	+	+	+
meso-Inositol	+	+	-
D-Lactose	+	-	+
D-Maltose	+	+	+
D-Mannitol	+	+	+
D-Mannose	+	+	+
D-Raffinose	+	+	-
$\alpha$ -L-Rhamnose	Not done	+	+
D-Sorbitol	-	-	-
Starch	+	+	No data
D-Sucrose	+	-	-
D-Xylose	-	+	-
CM-cellulose (0.1%, w/v)	-	-	No data
Sodium acetate (0.1%, w/v)	+	-	-
Sodium citrate (0.1%, w/v)	+	-	-
L-Arabinose	+	+	+
D-Fructose	+	+	+
D-Galactose	+	+	+
D-Glucose	+	+	+
meso-Inositol	+	+	-
D-Lactose	+	-	+
D-Maltose	+	+	+
Production of:			
Hydrogen sulphide	-	-	No data

<sup>a</sup>Numbers in parentheses indicate the diameters of the inhibition zones (mm). <sup>b</sup>*S. malaysiensis* DSM 41697<sup>T</sup> (data from Al-Tai *et al.* [53]), *S. samsunensis* M1463<sup>T</sup> (data from Sazak *et al.* [54]).

**Table 3.** 16S rDNA similarity values between strain W14 and its relatives of the genus *Streptomyces*.

<i>Streptomyces</i> species	Similarity to strain W14	No. nucleotide differences/Total no. nucleotides compared
<i>S. malaysiensis</i> NBRC 16446	99.65	5/1436
<i>S. samsunensis</i> M1463	99.64	5/1418
<i>S. asiaticus</i> NBRC 100774	98.54	21/1443
<i>S. rhizosphaericus</i> NBRC 100778	98.54	21/1443
<i>S. hygroscopicus</i> subsp. <i>azalomyceticus</i> NBRC 13868	98.54	21/1442
<i>S. griseiniger</i> NRRL B-1865	98.39	23/1436
<i>S. cangkringensis</i> DSM 41769	98.31	24/1422
<i>S. sporoclivatus</i> NBRC 100767	98.26	25/1442
<i>S. yatensis</i> NBRC 101000	98.19	26/1443
<i>S. castelarensis</i> subsp. <i>enhygrus</i> NRRL 3664	98.12	27/1443

Thus, based on results of the phenotypic and genotypic analysis, the strain W14 represents a novel species of the genus *Streptomyces*, for which we propose the name *Streptomyces zerumbet* sp. nov.

### 3.2. Isolation and Structure Elucidation of Bioactive Compounds

The partial components of crude extract were observed by TLC analysis in a solvent system comprising of acetone: hexane (2:3). The analysis of the separated compounds under UV light (254 and 365 nm) and upon derivatizing the TLC with vanillin/sulfuric acid reagent, revealed at least seven major spots with Rf values of 0.07, 0.20, 0.33, 0.46, 0.67, 0.77 and 0.91. In order to find out the correlation of these spots with antimicrobial property, bioautography of the freshly developed air-dried TLC strips containing separated components of the extract was performed, using *B. cereus*, *B. subtilis* and *S. aureus* as tested microorganisms. The results exhibited that the strain W14 produced at least one compound with Rf values of 0.67 against tested bacteria (**Figure 3**).

Column chromatography on silica gel with acetone: hexane as the mobile phase resulted in the separation of two major compounds. Identification of each compound was carried out by <sup>1</sup>H-NMR, <sup>13</sup>C-NMR as following.

Compound 1: The MS gave a [M + Na]<sup>+</sup> ion at *m/z* 179.0287 which corresponded to the molecular formula C<sub>7</sub>H<sub>8</sub>O<sub>4</sub>, indicating three double bond equivalents in the molecule. The <sup>1</sup>H-NMR spectral data (CDCl<sub>3</sub>) of compound 1 showed methoxy proton at δ<sub>H</sub> 3.88 (3H, s), oxygenated methine at δ<sub>H</sub> 4.66 (2H, s), two furan protons at δ<sub>H</sub> 6.42 (1H, d, *J* = 3.3 Hz) and 7.21 (1H, d, *J* = 3.3 Hz) ppm. The <sup>13</sup>C-NMR spectrum exhibited 7 signals which were classified by the HMQC spectra as methoxy carbon at δ<sub>C</sub> 52.2, oxygenated methine at δ<sub>C</sub> 57.7, two furan carbons at δ<sub>C</sub> 109.0 (C-4) and δ<sub>C</sub> 119.0 (C-3), two quaternary furan carbons at δ<sub>C</sub> 144.3 (C-2) and δ<sub>C</sub> 158 (C-5) and carbonyl ester at δ<sub>C</sub> 159.4 ppm.

The  $^1\text{H}$ - $^1\text{H}$  COSY spectrum revealed the connectivity in  $\text{CDCl}_3$  from H-3 through H-4. The HMBC spectrum showed the following long-range correlation; methoxy proton ( $\delta_H$  3.88) to ester carbonyl carbon C-1 ( $\delta$  159.4); oxygenated methine ( $\delta$  4.66) to quarternary furan carbon C-5 ( $\delta$  158.6) and furan carbon C-4 ( $\delta$  109.7); furan proton C-4 ( $\delta$  6.42) to quarternary furan carbon C-5 ( $\delta$  158.6), furan carbon C-3 ( $\delta$  119.1) and quarternary furan carbon C-2 ( $\delta$  144.3) and furan proton C-3 ( $\delta$  7.12) to quarternary furan carbon C-2 ( $\delta$  144.3), furan carbon C-4 ( $\delta$  109.7) and quarternary furan carbon C-5 ( $\delta$  158.6). The spectral data revealed the compound **1** to be methyl 5-(hydroxymethyl)furan-2-carboxylate (**Figure 4**). Its  $^1\text{H}$ - and  $^{13}\text{C}$ -NMR spectral data of which were in good agreement with those of furanoid toxin (**Table 4**) from *Curvularia lunata* which previously reported by Liu *et al.* [11].

**Compound 2:** The IR spectrum displayed characteristic absorption bands of NH and OH stretches at  $n$  3478, 3440, 3336 and 3297  $\text{cm}^{-1}$ , CH stretch in  $\text{CH}_3$  and  $\text{CH}_2$  at  $n$  2927  $\text{cm}^{-1}$ , CH stretch in methyl ether at  $n$  2853  $\text{cm}^{-1}$ , C=O stretch in  $\text{OCONH}_2$  at  $n$  1729  $\text{cm}^{-1}$ , C=O stretch in a,b-unsaturated amide at  $n$  1701  $\text{cm}^{-1}$  and C = O stretches in quinone at  $n$  1675 and 1652  $\text{cm}^{-1}$ . The MS gave a  $[\text{M}+\text{Na}]^+$  ion at  $m/z$  583.2571 which corresponded to the molecular formula  $\text{C}_{29}\text{H}_{40}\text{N}_2\text{O}_9$  for the compound, indicating eleven double bond equivalents in the molecule. The structure was fully elucidated by  $^1\text{H}$  NMR,  $^{13}\text{C}$  NMR spectroscopy, DEPT-135, and 2D NMR spectral studies. The  $^1\text{H}$ -NMR spectral data (DMSO-*d*<sub>6</sub>) of compound **2** showed four methyl groups at  $\delta_H$  0.75 (3H,  $J$  = 6.8 Hz), 0.97 (3H, brs), 1.62 (3H, s) and 1.93 (3H, s) three methoxy protons at  $\delta_H$  3.23 (3H, s), 3.24 (3H, s) and 3.96 (3H, s), five olefin protons at  $\delta_H$  5.50 (1H, d,  $J$  = 8.5 Hz), 5.81 (1H, br), 6.58 (1H, t), 6.95 (1H, d) and 7.04 (1H, s), four oxygenated methines at  $\delta_H$  3.09 (2H, br), 4.36 (1H, d,  $J$  = 7.6 Hz) and 4.88 (1H, br), amine hydrogen at  $\delta_H$  9.18 (1H, br), two methanefriyl group at  $\delta_H$  1.93 (1H, s)

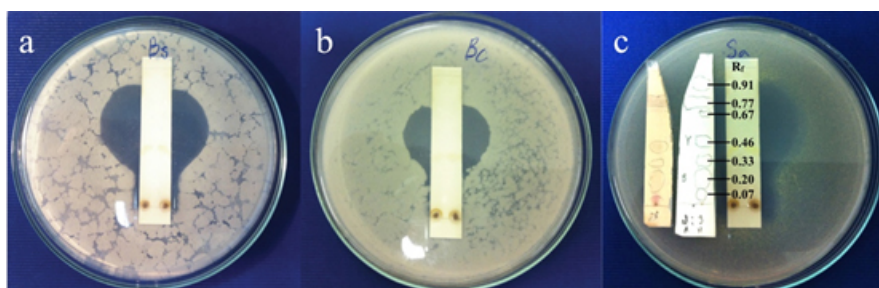


**Figure 3.** Bioautography technique for antibacterial activity of crude extract of the strain W14 against *Bacillus subtilis* ATCC 6633 (a), *B. cereus* ATCC 7064 (b), and *S. aureus* ATCC 25932 (c), on nutrient agar after 24 h of incubation at 37°C.

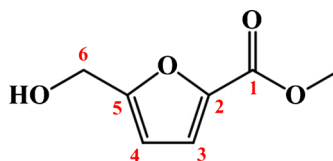


**Figure 4.** Chemical structures of methyl 5-(hydroxymethyl)furan-2-carboxylate (**1**).

and 2.56 (1H) and methanediyl groups at  $\delta_H$  1.45 (2H, br), 2.18 (1H, dd,  $J = 4.8$  and 12.5 Hz) and 2.43 (1H, dd,  $J = 9.9$  and 12.5 Hz) ppm. The  $^{13}\text{C}$ -NMR spectrum exhibited 39 signals which were classified by the DEPT-135 and HMQC spectra as four methyl carbons at  $\delta_C$  12.8 (2-Me), 13.0 (8-Me), 13.4 (8-Me) and 23.9 (14-Me), three methoxy carbons at  $\delta_C$  56.5 (12-OMe), 57.1 (6-OMe), and 61.6 (17-OMe), five olefin carbons at  $\delta_C$  111.3 (C-19), 126.3 (C-4), 128.7 (C-3), 132.4 (C-9) and 138.7 (C-5), five quaternary olefin carbons at  $\delta_C$  128.7 (C-16), 129.1 (C-8), 133.2 (C-2), 140.1 (C-20) and 156.9 (C-17), two methanetriyl carbons at  $\delta_C$  27.1 (C-14) and 32.6 (C-10), two methanediyl carbons at  $\delta_C$  31.3 (C-13) and 32.2 (C-15), four oxygenated methines at  $\delta_C$  72.4 (C-11), 80.7 (C-12), 81.1 (C-7) and 82.3 (C-6), four carbonyl carbons at  $\delta_C$  156.6 (7- $\text{OCONH}_2$ ), 169.7 (C-1), 183.6 (C-21) and 184.3 (C-18). The  $^1\text{H}$ - $^1\text{H}$  COSY spectrum revealed the connectivity, in DMSO- $d_6$  from H-3 through H-4; H-4 through H-3 and H-5; H-5 through H-4 and H-6; H-6 through H-5 and H-7; H-7 through H-6; H-9 through H-10; H-12 through H-9 and 10-Me; 10-Me through H-10; H-12 through H-13; H-13 through H-12 and H-14; H-14 through H-13, 14-Me and H-15; 14-Me through H-14 and H-15 through H-14. The HMBC spectrum showed the following long-range correlations; 2-Me ( $\delta_H$  1.93) to C-1 ( $\delta_C$  169.7), C-2 ( $\delta_H$  133.2) to C-3 ( $\delta_C$  128.7) and C-4 ( $\delta_C$  126.3); H-4 ( $\delta_H$  6.58) to C-2 ( $\delta_C$  133.2) and C-6 ( $\delta_C$  82.3); H-6 ( $\delta_H$  4.36) to C-4 ( $\delta_C$  126.3), 6-OMe ( $\delta_C$  57.1); 6-OMe ( $\delta_H$  3.24) to C-6 ( $\delta_C$  82.3); H-7 ( $\delta_H$  4.88) to C-5 ( $\delta_C$  138.7), 7- $\text{OCONH}_2$  ( $\delta_C$  156.6), C-9 ( $\delta_C$  132.4) and 8-Me ( $\delta_C$  13.0); 8-Me ( $\delta_H$  1.62) to C-7 ( $\delta_C$  81.1) and C-9 ( $\delta_C$  132.4); H-9 ( $\delta_H$  5.50) to C-7 ( $\delta_C$  81.1), and 8-Me ( $\delta_C$  13.0); 10-Me ( $\delta_H$  0.75) to C-9 ( $\delta_C$  132.4), C-10 ( $\delta_C$  32.6), and C-11 ( $\delta_C$  72.4); H-11 ( $\delta_H$  3.09) to 10-Me ( $\delta_C$  13.4); H-12 ( $\delta_H$  3.09) to 12-OMe ( $\delta_C$  56.5); 12-OMe ( $\delta_H$  3.23) to C-12 ( $\delta_C$  80.7); H-13 ( $\delta_H$  1.45) to 14-Me ( $\delta_C$  23.9); H-14 ( $\delta_H$  1.93) to C-12 ( $\delta_C$  80.7) and C-16 ( $\delta_C$  128.7); 14-Me ( $\delta_H$  0.97) to C-14 ( $\delta_C$  27.1) and C-15 ( $\delta_C$  32.2); H-15 ( $\delta_H$  2.18, 2.43) to C-13 ( $\delta_C$  31.3), C-14 ( $\delta_C$  27.1), C-16 ( $\delta_C$  128.7), C-17 ( $\delta_C$  156.9) and C-21 ( $\delta_C$  183.6); 17-OMe ( $\delta_H$  3.96) to C-17 ( $\delta_C$  156.9) and NH ( $\delta_H$  9.18) to C-1 ( $\delta_C$  169.7), C-19 ( $\delta_C$  111.3) and C-21 ( $\delta_C$  183.6). The spectral data revealed the compound **2** to be geldanamycin (**Figure 5**). Its  $^1\text{H}$ - and

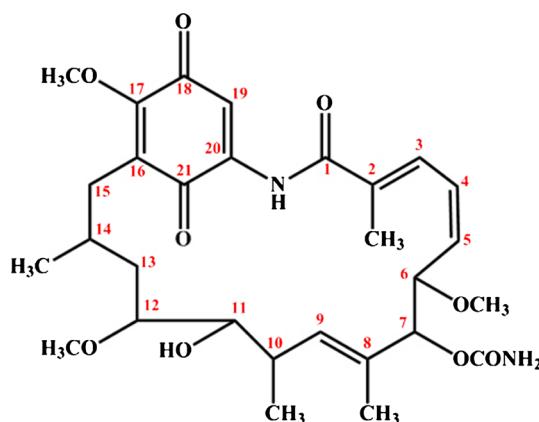


**Figure 5.** Chemical structures of and geldanamycin (**2**).

$^{13}\text{C}$ -NMR spectral data of which were in good agreement with those of geldanamycin (**Table 5**) previously reported by Ōmura *et al.* [12] and Qin and Panek [13].

### 3.3. Assessment of Cytotoxicity Activity of Crude Extract and Purified Compounds

Crude extract and purified compounds from *Streptomyces zerumbet* strain W14 were tested for their cytotoxic activities by MTT-assay on L929, RAW264.7, HeLa cells and PBMC. The  $\text{IC}_{50}$  values were exhibited in **Table 6**. *In vitro* cytotoxicity assays revealed that crude extract exhibited cytotoxicity against RAW264.7 cells and moderated cytotoxicity against L929 and PBMC. The activity of compounds **1** and **2** against RAW264.7 cells exhibited less toxicity with  $\text{IC}_{50} > 512 \mu\text{g/ml}$ . However, compound **1** showed cytotoxic activity on HeLa cells and moderate activity to L929 cells, while compound **2** exhibited a cytotoxic activity on PBMC.

### 3.4. Antibacterial Activity of Purified Compounds

Purified compounds from *Streptomyces zerumbet* strain W14 were tested for their antibacterial activity by MIC and MBC methods. Results in **Table 7** showed that compound **1** was the most active against tested bacterial strains. It showed the highest activity against *S. aureus* with MIC and MBC values of  $1 \mu\text{g/ml}$  and  $16 \mu\text{g/ml}$ , respectively, followed active against MRSA (clinical isolate) with MIC and MBC values of  $1 \mu\text{g/ml}$  and  $64 \mu\text{g/ml}$ , respectively. Interestingly, compound **1** was also active against Bacillus Calmette-Guérin (BCG), vaccine strain, with MIC and MBC values of  $128 \mu\text{g/ml}$  and  $128 \mu\text{g/ml}$ , respectively, while compound **2** showed low activity against tested bacterial strains with MIC and MBC values greater than  $512 \mu\text{g/ml}$ . Gentamicin  $10.00 \mu\text{g/ml}$  and rifampicin (for BCG)  $8.00 \mu\text{g/ml}$  were used as positive control.

**Table 4.** Comparison of the spectral data of the compound **1** and CF<sup>a</sup>.

No.	$\delta_{\text{C}}$ compound <b>1</b>	$\delta_{\text{C}}$ CF	$\delta_{\text{H}}$ compound <b>1</b>	$\delta_{\text{H}}$ CF	HMBC (H $\rightarrow$ C)	COSY
1	159.4, C	160.3, C	-	-	-	-
2	144.3, C	142.8, C	-	-	-	-
3	119.1, CH	119.0, CH	7.12 (d, 3.3)	7.21 (d, 3.4)	2, 4, 5	4
4	109.7, CH	109.0, CH	6.42 (d, 3.3)	6.44 (d, 3.4)	2, 3, 5	3
5	158.6, C	158.2, C	-	-	-	-
6	57.7, CH <sub>2</sub>	56.1, CH <sub>2</sub>	4.66 (s)	4.45 (d, 5.8)	4, 5	-
1-OMe	52.2, CH <sub>3</sub>	51.9, CH <sub>3</sub>	3.88 (s)	3.77 (s)	1	-
6-OH	-	-	-	5.80 (t, 5.8)	-	-

<sup>a</sup>CF, *Curvularia lunata* furanoid toxin (data from Liu *et al.*, [11]). <sup>1</sup>H and <sup>13</sup>C-NMR assignments for compound **1** [<sup>1</sup>H (300 MHz), <sup>13</sup>C-NMR (75 MHz), CDCl<sub>3</sub>, *J* = Hz]; *Curvularia lunata* furanoid toxin [<sup>1</sup>H (400 MHz), <sup>13</sup>C-NMR (400 MHz), DMSO-*d*<sub>6</sub>, *J* = Hz].

**Table 5.** Comparison of the spectral data of the compound **2** and GDA<sup>a</sup>.

No.	$\delta_C$ compound 2	$\delta_C$ GDA	$\delta_H$ compound 2	$\delta_H$ GDA	HMBC (H $\rightarrow$ C)	COSY	NOESY
1	169.7 C	169.1	-	-	-	-	-
2	133.2 C	133.2	-	-	-	-	-
2-Me	12.8 CH <sub>3</sub>	12.2	1.93 s	1.91 s	1, 2, 3, 4	-	-
3	128.7 CH	128.4	6.95 d	6.95 d	-	4	NH, 4, 6, 7
4	126.3 CH	125.7	6.58 t	6.56 t	2, 6	3, 5	3, 5
5	138.7 CH	137.8	5.81 br	5.80 t	-	4, 6	4, 6
6	82.3 CH	81.6	4.36 d (7.6)	4.34 d	4, 6-OMe	5, 7	3, 5, 7
6-OMe	57.1 CH <sub>3</sub>	56.0	3.24 s	3.22 s	6	-	-
7	81.1 CH	80.6	4.88 br	4.86 br	5, 7-OCONH <sub>2</sub> , 9, 8-Me	6	3, 6, 9
7-OCONH <sub>2</sub>	156.6 C	156.0	-	6.45 br	-	-	-
8	129.1 C	132.6	-	-	-	-	-
8-Me	13.0 CH <sub>3</sub>	12.5	1.62 s	1.61 s	7, 9	-	10
9	132.4 CH	131.9	5.50 d (8.5)	5.51 d	7, 8-Me	10	7
10	32.6 CH	32.1	2.56	3.61 m	-	9, 10-Me	8-Me, 10-Me, 11, 12
10-Me	13.4 CH <sub>3</sub>	23.3	0.75 d (6.8)	0.97 d	9, 10, 11	10	10, 11, 12
11	72.4 CH	71.9	3.09 br	3.29 s	10-Me	-	10, 10-Me, 13, 14
11-OH	-	-	-	-	-	-	-
12	80.7 CH	80.2	3.09 br	3.07 m	12-OMe	13	10, 10-Me, 13, 14
12-OMe	56.5 CH <sub>3</sub>	56.6	3.23 s	3.23 s	12	-	-
13	31.3 CH <sub>2</sub>	31.0	1.45 br	1.45 m	14-Me	12, 14	11, 12, 14
14	27.1 CH	26.6	1.93 s	1.91 br	12, 16	13, 14-Me, 15a, 15b	13
14-Me	23.9 CH <sub>3</sub>	13.0	0.97 br	0.76 d	14, 15	14	-
15a	32.2 CH <sub>2</sub>	31.7	2.43 dd (12.5, 9.9)	2.42 m	13, 14, 16, 17, 21	14, 15b	-
15b		31.7	2.18 dd (12.5, 4.8)		13, 14, 16, 17, 21	14, 15a	-
16	128.7 C	128.1	-	-	-	-	-
17	156.9 C	156.4	-	-	-	-	-
17-OMe	61.6 CH <sub>3</sub>	61.0	3.96 s	3.93 s	17	-	-
18	184.3 C	183.6	-	-	-	-	-
19	111.3 CH	110.9	7.04 s	7.02 s	-	-	-
20	140.1 C	139.6	-	-	-	-	-
21	183.6 C	183.1	-	-	-	-	-
NH	-	-	9.18 NH, br	9.14 NH, br	1, 19, 21	-	3

<sup>a</sup>GDA, geldanamycin (data from Ōmura *et al.*[12]). <sup>1</sup>H and <sup>13</sup>C-NMR assignments for compound **2** [<sup>1</sup>H (400 MHz), <sup>13</sup>C-NMR (100 MHz), DMSO-*d*<sub>6</sub>, *J* = Hz]; Geldanamycin [<sup>1</sup>H, <sup>13</sup>C-NMR, DMSO-*d*<sub>6</sub>, *J* = Hz].

**Table 6.** IC<sub>50</sub> of the crude extract and purified compounds against diiference cell lines after 24 using the MTT assay.

Test agents	IC <sub>50</sub> <sup>a</sup> (µg/ml)			
	L929 <sup>b</sup>	PBMC	RAW 264.7	HeLa
Crude extract	108.85	165.31	4.67	- <sup>c</sup>
Compound 1	239.06	1097.07	>512.00	64.00
Compound 2	1372.23	52.23	>512.00	>512.00

<sup>a</sup>IC<sub>50</sub> values represent the concentration causing 50% growth inhibition. They were determined by linear regression analysis. <sup>b</sup>L929, murine fibroblast cell line; PBMC, human peripheral blood mononuclear cells; RAW 264.7, murine macrophage cell line; HeLa, human cervical carcinoma cell line. <sup>c</sup>-, Not determine.

**Table 7.** Antibacterial activity of compound 1.

Bacteria	Concentration (µg/ml)	
	MIC	MBC
<i>Staphylococcus aureus</i> ATCC 25923	1.00	16.00
MRSA	1.00	64.00
Bacillus Calmette-Guérin (BCG)	128.00	128.00

### 3.5. Effects of Purified Compounds on NO and PGE<sub>2</sub> Production in LPS-Induced RAW 264.7 Cells

LSP caused a significant increase in NO and PGE<sub>2</sub> production when compared with the blank control, only compound 2 caused a significant reduction in NO and PGE<sub>2</sub> production when compared with LPS-induced control group ( $p < 0.05$ ). In detail, the production of NO in LPS-induced RAW 264.7 incubated with compound 2 at concentrations of 1, 2.5 and 5 µg/ml for 24 h were  $48.72 \pm 7.43$ ,  $36.51 \pm 5.84$  and  $20.28 \pm 4.66$  µM, respectively, and the production of PGE<sub>2</sub> were  $40.74 \pm 6.05$ ,  $26.62 \pm 6.83$  and  $20.77 \pm 4.48$  ng/ml, respectively, while the production of NO and PGE<sub>2</sub> in the group treated with LPS only was  $52.64 \pm 6.11$  µM and  $51.75 \pm 6.56$  ng/ml, respectively. Therefore, the inhibitory levels of compound 2 on NO and PGE<sub>2</sub> production also showed a dose-dependent pattern (**Figure 6** (NO) and **Figure 7** (PGE<sub>2</sub>)), while compound 1 did not cause a significant reduction in NO and PGE<sub>2</sub> production on LPS-induced RAW 264.7 cells at the concentration of 1 to 5 µg/ml (data not shown). Since compound 2 has inhibitory effect on NO and PGE<sub>2</sub> production in LPS-induced RAW 264.7. It was considered on the test of inhibitory effects on iNOS and COX-2 production, proinflammatory cytokine production and also up-regulation of gene expression in LPS-induced RAW 264.7.

### 3.6. Effects of Compound 2 on iNOS and COX-2 Production in LPS-Induced RAW 264.7 Cells

The effects of compound 2 on iNOS and COX-2 production in LPS-induced RAW 264.7 cells were also carried out by Western blot analysis. Results of relative density ratio from Western blot analysis further indicated that iNOS and

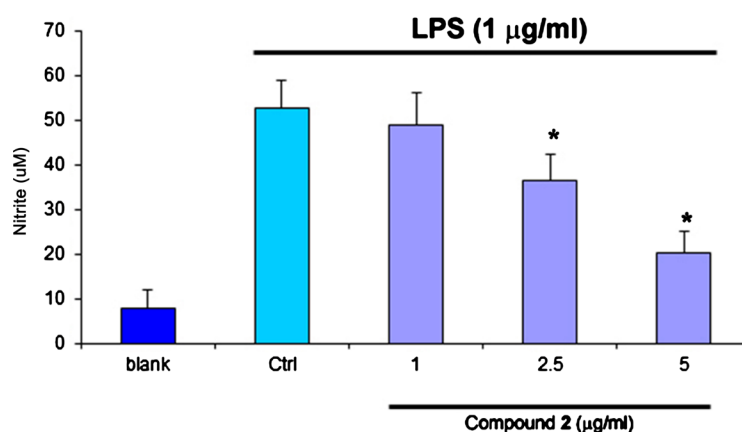


**Figure 6.** Evaluation of nitrite production by RAW 264.7 cells stimulated for 24 h with LPS alone or in combination with increasing concentrations (1 - 5 µg/ml) of compound **2**. The values are the means of at least three determinations  $\pm$  SEM. Probability level (Student's *t*-test): \* $p < 0.05$  vs. LPS-treated group.

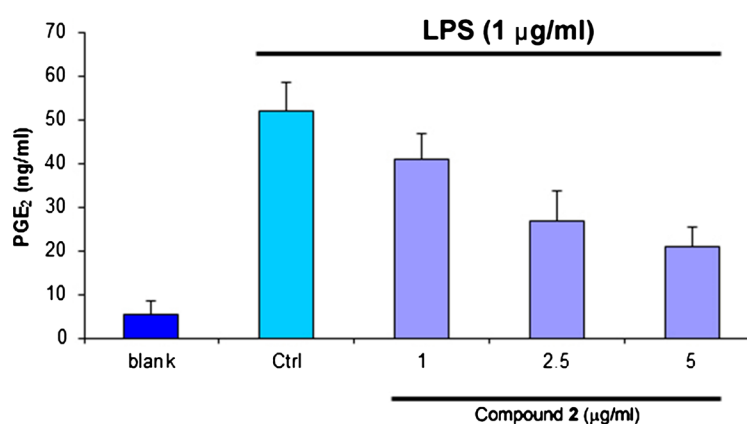


**Figure 7.** Effect of compound **2** on PGE<sub>2</sub> production in LPS-induced RAW 264.7 macrophage for 24 h. The values are the means of at least three determinations  $\pm$  SEM. Probability level (Student's *t*-test).

COX-2 production in LPS-induced RAW 264.7 cells were significantly reduced when treated with purified compounds in different concentration (**Figure 8**). In detail, the relative density ratio of iNOS production in LPS-induced RAW 264.7 incubated with compound **2** at concentrations of 1, 2.5 and 5 µg/ml for 24 h were 84.67, 60.83 and 41.82, respectively, and the relative density ratio of COX-2 production in LPS-induced RAW 264.7 were 81.89, 56.86 and 34.79, respectively. Therefore, the inhibitory levels of compound **2** on iNOS and COX-2 production in LPS-induced RAW 264.7 cells also showed a dose-dependent pattern.

### 3.7. Effects of Compound **2** on Pro-Inflammatory Cytokine Production in LPS-Induced RAW 264.7 Cells

In this study, data showed that compound **2** decreased production of pro-inflammatory cytokines such as TNF- $\alpha$ , IL-1 $\beta$  and IL-6 in LPS-induced RAW 264.7 cells ( $p < 0.05$ ) (**Figures 9-11**). Treatment with LPS alone in RAW 264.7 cells resulted in a significant increase of pro-inflammatory cytokine productions compared with



the blank control group. The detailed results of this assay are as follows: TNF- $\alpha$  productions in LPS-induced RAW 264.7 cells incubated with compound **2** at concentrations of 1, 2.5 and 5  $\mu\text{g/ml}$  for 24 h were  $36.56 \pm 5.51$ ,  $22.79 \pm 4.80$  and

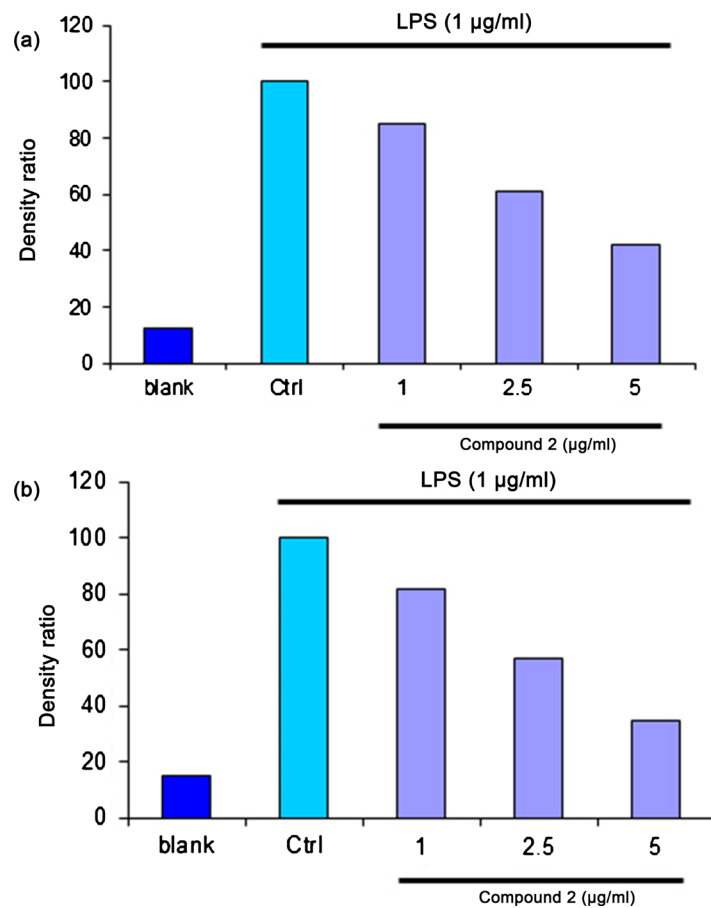


**Figure 8.** Effect of compound **2** on iNOS protein production (a) and COX-2 protein expression (b) by LPS-induced RAW 264.7 macrophage for 24 h. Probability level (Student's *t*-test): \* $p < 0.05$  vs. LPS-treated group.

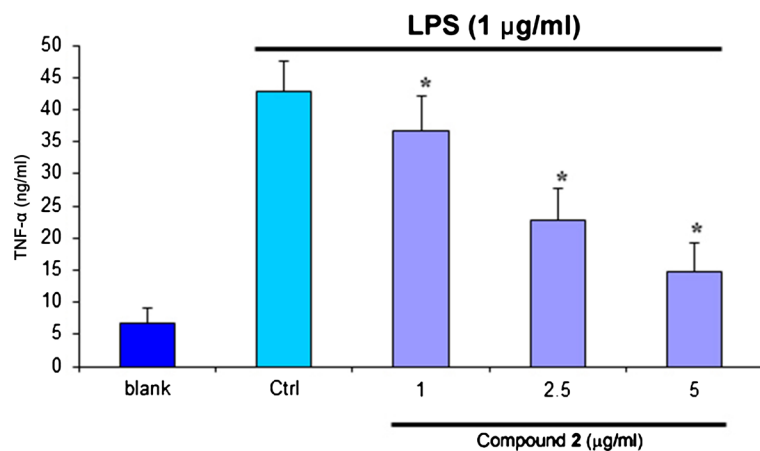


**Figure 9.** Effect of compound **2** on LPS-induced TNF- $\alpha$  production by RAW 264.7 cells. The values are the means of at least three determinations  $\pm$  SEM. Probability level (Student's *t*-test): \* $p < 0.05$  vs. LPS-treated group.

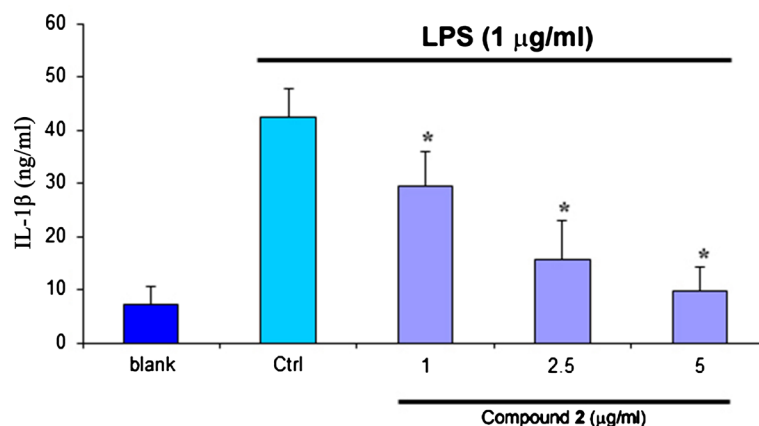


**Figure 10.** Effect of compound 2 on LPS-induced IL-1 $\beta$  production by RAW 264.7 cells. The values are the means of at least three determinations  $\pm$  SEM. Probability level (Student's *t*-test): \**p* < 0.05 vs. LPS-treated group.

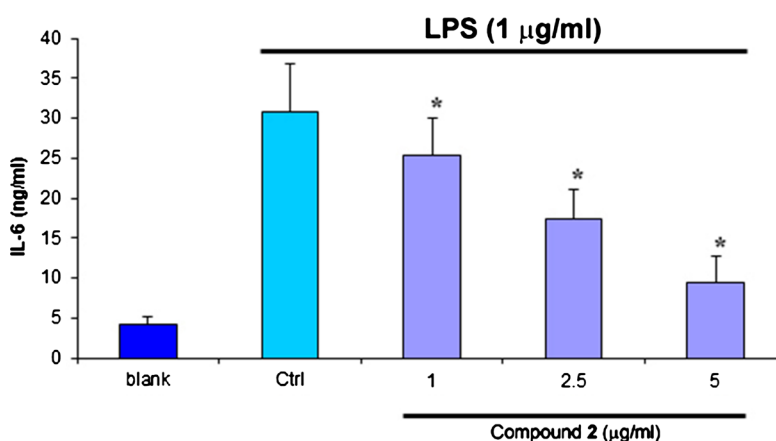


**Figure 11.** Effect of compound 2 on LPS-induced IL-6 production by RAW 264.7 cells. The values are the means of at least three determinations  $\pm$  SEM. Probability level (Student's *t*-test): \**p* < 0.05 vs. LPS-treated group.

14.73  $\pm$  4.52 ng/ml, respectively, IL-1 $\beta$  productions in LPS-induced RAW 264.7 cells incubated with compound 2 at different concentrations were 29.57  $\pm$  6.28, 15.64  $\pm$  7.26 and 9.62  $\pm$  4.58 ng/ml, respectively, and IL-6 productions in LPS-induced RAW 264.7 cells incubated with compound 2 at different concentrations were 25.37  $\pm$  4.62, 17.45  $\pm$  3.67 and 9.46  $\pm$  3.34 ng/ml, respectively. Therefore, treatment with compound 2 (1 - 5  $\mu$ g/ml) clearly inhibited the production of TNF- $\alpha$ , IL-1 $\beta$  and IL-6 in a dose-dependent manner in LPS-induced RAW 264.7 cells.

### 3.8. Effects of Compound 2 on Up-Regulation of iNOS and Proinflammatory Cytokine Transcriptions in LPS-Induced RAW 264.7 Cells

Since compound 2 inhibited the production of NO and proinflammatory cytokines, the correlation between the concentration of compound 2 and the mRNA expression of iNOS and proinflammatory cytokines was investigated. RAW

264.7 cells were pretreated with different concentrations (1 - 10  $\mu\text{g/ml}$ ) of compound **2** for 2 h and then incubated with or without 1  $\mu\text{g/ml}$  of LPS for 6 h, total mRNA was isolated, and the mRNA levels of iNOS and proinflammatory cytokines were examined by RT-PCR. Treatment with LPS also significantly increased the mRNA expression levels of iNOS and proinflammatory cytokines (Figure 12). However, this induction of iNOS and proinflammatory cytokines mRNA expression was significantly inhibited by 5  $\mu\text{g/ml}$  of compound **2**. In addition, pretreatment with 10  $\mu\text{g/ml}$  of compound **2** significantly inhibited this upregulation of iNOS and proinflammatory cytokines mRNA expression, particularly of IL-1 $\beta$  and IL-6 mRNA expression.

#### 4. Discussion

Strain W14 was isolated from the rhizome tissue of *Zingiber zerumbet* (L.) Smith, a medicinal plant containing several compounds, for example, polyphenols, alkaloids and terpenes [14]. This microbe produced secondary metabolites after inoculation onto ISP-2 medium for 14 days. Based on morphological observation as well as on the presence of LL-type diaminopimelic acid in the whole-cell extracts and 16S rDNA sequence, the strain W14 was identified as belonging to the genus *Streptomyces*. Although, the level of 16S rDNA sequence similarity between this isolate and the type strain (*S. malaysiensis*) of its closest relatives in the genus *Streptomyces* was 99.65%, but the physiological characterization clearly differentiated this isolate from its closest neighbours, implying that this isolate was distinctive. It is therefore concluded that this isolate represents a novel species of the genus *Streptomyces*, for which the name *Streptomyces zerumbet* is proposed.

Two major compounds were isolated from the *Streptomyces zerumbet* W14 crude extract, and were identified to be methyl 5-(hydroxymethyl)furan-2-carboxylate (**1**) and geldanamycin (**2**). To the best of our knowledge, compound **1** is furanoid toxin, which had been isolated from *Curvularia lunata*, the pathogen that causes *Curvularia* leaf spot on maize [11]. This compound has been synthesized and shown antibacterial activity with MIC value of 100  $\mu\text{g/ml}$  against *Streptococcus*

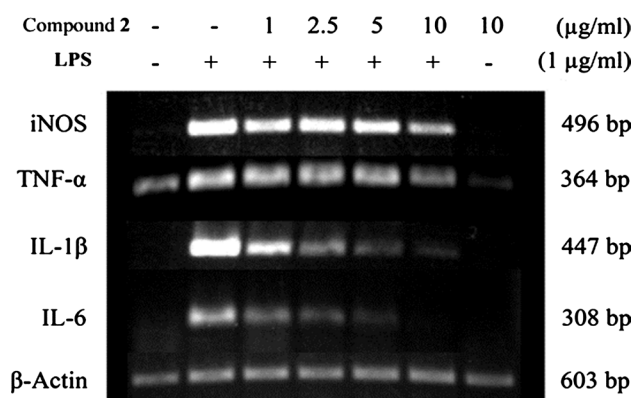


**Figure 12.** Effect of compound **2** on LPS-induced mRNA expression of inducible nitric oxide synthase (iNOS) and proinflammatory cytokines in RAW 264.7 cells.

*pyogenes*, *Proteus vulgaris*, and *E. coli* [15]. In this study, compound 1 exhibited better antibacterial activity especially towards *S. aureus* ATCC 25923 with MIC and MBC values of 1.00 µg/ml and 16.00 µg/ml, respectively. It also exhibited significant cytotoxicity against HeLa cells with IC<sub>50</sub> value of 64 µg/ml. The results were in agreement with furan-2-carboxylic acid, 5-3-(hydroxymethyl)-4,5-dimethoxyphenyl]-3-methylfuran-2-carboxylic acid isolated from the bark of *Cassia alata*, which displayed cytotoxicity against NB4 (acute promyelocytic leukemia cell line), A549 (adenocarcinomic alveolar basal epithelial cell line), SHSY5Y (neuroblastoma cell line), PC3 (prostate cancer cell line) and MCF7 (breast adenocarcinoma cell line) cell lines with IC<sub>50</sub> values of 2.5, 1.2, 2.2, 3.6 and 1.9 µmol/l, respectively [16]. Compound 2 (geldanamycin) had been discovered in the culture filtrates of *Streptomyces hygrosopicus* var. *geldanus* var. *nova*. It was moderately active *in vitro* against protozoa, bacteria and fungi [17]. In this study, it exhibited low antibacterial activity with MIC and MBC values greater than 512 µg/ml. It also exhibited significant cytotoxicity against PBMC, but no cytotoxicity against L929, RAW 264.7 and HeLa cells which differed from those reports of geldanamycin was extremely active against KB cells; an ubiquitous keratin-forming HeLa cell line (<0.001 µg/ml), L1210 cells; a mouse lymphocytic leukemia cell line (<0.002 µg/ml) [17], SKBr3; a human breast cancer cell line (IC<sub>50</sub> value of 37 nM) [18] and A431; human epidermoid carcinoma cell line and BC; breast cancer cell line with IC<sub>50</sub> value of 0.15 and 0.01 µg/ml, respectively [19].

During our investigations of the anti-inflammatory compounds, biphenyls were isolated from *Streptomyces* sp. BO-07 which had anti-inflammatory activities [20]. Geldanamycin has been reported as a potent anti-inflammatory compound that target heat-shock protein 90 and glucose-related protein 96 [21] [22], which act as intracellular chaperones that maintain the structural integrity of cytoplasmic and endoplasmic reticulum-associated proteins, respectively. It binds to, and inactivates the function of, an Hsp90-Hsp70 multichaperone machine [23]. This multisubunit complex maintains the conformation and activity of regulatory kinases (e.g. c-src, cyclin-dependent protein kinase 4 [CDK4], Raf-1, and p38) [24] [25] [26], and nitric oxide synthase (NOS) [27] in eukaryotic cells. Because several Hsp90 substrates promote cellular activation and cell growth by maintaining the structural integrity of kinases such as c-Src, Raf-1, CDK4, extracellular signal-regulated kinase 1, JNK, p38 MAPK, lymphocyte-specific protein tyrosine kinase, protein kinase R [28] [29] [30] [31], and transcription factors (e.g. NF-κB), steroid hormone receptors [32] [33] [34], these proteins have potent antiproliferative effects both *in vitro* and *in vivo* [35]. Other Hsp90 substrates (e.g. NOS) promote inflammation. Because of this, geldanamycin has potent anti-inflammatory effects [36] [37] by binding to the amino-terminal ATPase domain of Hsp90 and inactivates its function [21] [38]. Inhibition of the function of Hsp90 substrates with the use of geldanamycin has antiproliferative and anti-inflammatory effects [22] [39] [40] [41] [42]. Thus, the anti-inflammatory effects of geldanamycin are produced, in part, by inhibiting

the production of pro-inflammatory cytokines such as TNF- $\alpha$ , IL-1 $\beta$  and IL-6, and pro-inflammatory mediator such as NO and PGE<sub>2</sub>, and also iNOS and COX-2 in LPS-induced RAW 264.7 cells were investigated.

Our results indicate that compound **2** inhibits the TNF- $\alpha$ , IL-1 $\beta$  and IL-6 mRNA transcription. The results were in agreement with geldanamycin inhibits the production of TNF- $\alpha$  in taxol, LPS, or CpG DNA-activated RAW 264.7 cells [43] [44], indicating that compound **2** has more general anti-inflammatory properties. This is consistent with a previous report showing that inhibition of Hsp90 by radicicol (which its structure related to geldanamycin) repressed the mRNA transcription TNF- $\alpha$ , IL-1 $\beta$  and IL-6 genes in LPS-stimulated THP-1 cells, a human macrophage-like cell line [45] and geldanamycin inhibited the translation of TNF- $\alpha$  and IL-6 transcription in LPS-activated RAW 264.7 cells, but did not appear to inhibit the translation of IL-1 $\beta$  [46], which was difference from this study. This is important because previous work by Wax *et al.* [46] showed that a low dose of geldanamycin (300 nM). In contrast, the higher does of geldanamycin (5  $\mu$ g/ml) used in this study inhibit the transcription and translation of the pro-inflammatory cytokines. Furthermore, compound **2** also suppressed the expression of COX-2 and iNOS induced by LPS, implying that this compound activation negatively regulates the expression of these pro-inflammatory mediators. Our results indicate that Hsp90 is critical to the transcriptional control of these pro-inflammatory cytokines and mediators in LPS-activated macrophages. It is thus possible that the function of Hsp90 is also critical to inflammatory cytokine and mediator production in autoimmune inflammatory diseases and that inhibition of Hsp90 could be a useful target for future drug development.

In addition, previous work by Igarashi *et al.* [47] showed that zerumbone (which its structure related to radicicol and geldanamycin) in *Zingiber zerumbet* Smith, increased cellular protein aggregates and promoted nuclear translocation of heat shock factor 1 (HSF1), which down-regulation attenuated the suppressive effects of zerumbone on mRNA and protein expressions of pro-inflammatory genes, including inducible nitric oxide synthase and IL-1 $\beta$ . In this study, geldanamycin isolated from *Streptomyces zerumbet*, an endophyte of *Zingiber zerumbet*, has structure related to zerumbone from *Zingiber zerumbet*. Since, some endophyte promoted the accumulation of secondary metabolites of host plants, which influenced the quantity and quality of compounds, or could produce diverse classes of phytochemicals, secondary metabolites originally from plants, including the structural analog compounds [48] [49] [50] [51] [52]. It was suggested that compound relationship between endophyte and host plants should be further studied in the future. This knowledge can be applied for the production of better and new drugs from endophytes and their medicinal plants.

The results obtained here demonstrate that *Streptomyces zerumbet*, a novel species isolated from *Zingiber zerumbet* (L.) Smith could produce methyl 5-(hydroxymethyl)furan-2-carboxylate (**1**) and geldanamycin (**2**). The compound **1** had antibacterial activity against *Staphylococcus aureus* ATCC 25923 and

Methicillin-resistant *S. aureus* with the MIC and MBC values of 1 µg/ml and 16 - 64 µg/ml, respectively, while the compound **2** at the concentration of 1 - 5 µg/ml had *in vitro* anti-inflammatory activity on LPS-induced RAW 264.7 cells by inhibition of mRNA expression and production of inducible NO synthase (iNOS), nitric tumor necrosis factor- $\alpha$  (TNF- $\alpha$ ), interleukin-1 $\beta$  (IL-1 $\beta$ ), and interleukin-6 (IL-6). These results indicate that the compounds **1** and **2** exhibited promising antibacterial and anti-inflammatory activities, respectively. In conclusion we suggest that the future studies on these compounds could be useful for the management of bacterial infections and inflammatory diseases. And the compound relationship between endophyte and host plants should be also further studied in the future.

### Acknowledgements

The authors are grateful to Ms Sopita Rattanopas and Ms Siwaporn Inpang in the Department of Chemistry, Faculty of Science, Silpakorn University, Thailand, for measuring NMR and MS data, respectively. This work was supported by the Higher Education Research Promotion and National Research University Project of Thailand, Office of the Higher Education Commission, Thailand.

### Conflicts of Interest

The authors declare no conflicts of interest regarding the publication of this paper.

### References

- [1] Taechowisan, T. and Lumyong, S. (2003) Activity of Endophytic Actinomycetes from Roots of *Zingiber officinale* and *Alpinia galanga* against Phytopathogenic Fungi. *Annals of Microbiology*, **53**, 291-298.
- [2] Taechowisan, T., Lu, C.H., Shen, Y.M. and Lumyong, S. (2005) 4-Arylcoumarins from Endophytic *Streptomyces aureofaciens* CMUAc130 and Their Antigungal Activity. *Annals of Microbiology*, **55**, 63-66.
- [3] Taechowisan, T., Peberdy, J.F. and Lumyong, S. (2003) Isolation of Endophytic Actinomycetes from Selected Plants and Their Antifungal Activity. *World Journal of Microbiology and Biotechnology*, **19**, 381-385. <https://doi.org/10.1023/A:1023901107182>
- [4] Taechowisan, T., Chaisaeng, S. and Phutdhawong, W.S. (2017) Antibacterial, Antioxidant and Anticancer Activities of Biphenyls from *Streptomyces* sp. BO-07: An Endophyte in *Boesenbergia rotunda* (L.) Mansf A. *Journal Food and Agricultural Immunology*, **28**, 1330-1346. <https://doi.org/10.1080/09540105.2017.1339669>
- [5] National Committee for Clinical Laboratory Standards (1997) Performance Standards for Antimicrobial Disk Susceptibility Tests. Approved Standard M2-A6. Wayne, PA.
- [6] National Committee for Clinical Laboratory Standards (2000) Methods for Dilution Antimicrobial Susceptibility Tests for Bacteria That Grow Aerobically. Approved standard M7-A5. Wayne, PA.
- [7] Grievink, H.W., Luisman, T., Kluff, C., Moerland, M. and Malone, K.E. (2016)

- Comparison of Three Isolation Techniques for Human Peripheral Blood Mononuclear Cells: Cell Recovery and Viability, Population Composition, and Cell Functionality. *Biopreservation and Biobanking*, **14**, 410-415.  
<https://doi.org/10.1089/bio.2015.0104>
- [8] Green, L.C., Wagner, D.A., Glogowski, J., Skipper, P.L., Wishnok, J.S., *et al.* (1982) Analysis of Nitrate, Nitrite, and [<sup>15</sup>N]Nitrate in Biological Fluids. *Analytical Biochemistry*, **126**, 131-138. [https://doi.org/10.1016/0003-2697\(82\)90118-X](https://doi.org/10.1016/0003-2697(82)90118-X)
- [9] Taechowisan, T., Wanbanjob, A., Tuntiwachwuttikul, P. and Liu, J.K. (2009) Anti-Inflammatory Activity of Lansai C from Endophytic *Streptomyces* sp. SUC1 in LPS-Induced RAW 264.7 Cells. *Journal Food and Agricultural Immunology*, **20**, 67-77. <https://doi.org/10.1080/09540100902730064>
- [10] Brosius, J., Palmer, M.L., Kennedy, P.J. and Noller, H.F. (1978) Complete Nucleotide Sequence of a 16S Ribosomal RNA Gene from *Escherichia coli*. *Proceedings of the National Academy of Sciences of the United States of America*, **75**, 4801-4805.  
<https://doi.org/10.1073/pnas.75.10.4801>
- [11] Liu, T., Liu, L.X., Jiang, X., Huang, X.L. and Chen, J. (2009) A New Furanoid Toxin Produced by *Curvularia lunata*, the Causal Agent of Maize Curvularia Leaf Spot. *Journal Canadian Journal of Plant Pathology*, **31**, 22-27.  
<https://doi.org/10.1080/07060660909507568>
- [12] Ōmura, S., Nakagawa, A. and Sadakane, N. (1979) Structure of Herbmicycin A New Ansamycin Antibiotic. *Tetrahedron Letters*, **20**, 4323-4326.  
[https://doi.org/10.1016/S0040-4039\(01\)86578-3](https://doi.org/10.1016/S0040-4039(01)86578-3)
- [13] Qin, H.L. and Panek, J.S. (2008) Total Synthesis of the Hsp90 Inhibitor Geldanamycin. *Organic Letters*, **10**, 2477-2479. <https://doi.org/10.1021/ol800749w>
- [14] Koga, A.Y., Beltrame, F.L. and Pereira, A.V. (2016) Several Aspects of *Zingiber zerumbet*: A Review. *Revista Brasileira de Farmacognosia*, **26**, 385-391.  
<https://doi.org/10.1016/j.bjp.2016.01.006>
- [15] Malladi, S., Nadh, R.V., Babu, K.S. and Babu, P.S. (2017) Synthesis and Antibacterial Activity Studies of 2,4-di Substituted Furan Derivatives. *Beni-Suef University Journal of Basic and Applied Sciences*, **6**, 345-353.
- [16] Zhou, L., Dong, W., Wang, Y., Zhou, K., Ma, H.Y., *et al.* (2016) A New Furan-2-Carboxylic Acid from Stem Bark of *Cassia alata*. *China Journal of Chinese Materia Medica*, **41**, 2652-2654.
- [17] Deboer, C., Meulman, P.A., Wnuk, R.J. and Peterson, D.H. (1970) Geldanamycin, a New Antibiotic. *Journal of Antibiotics*, **23**, 442-447.  
<https://doi.org/10.7164/antibiotics.23.442>
- [18] Hu, Z., Liu, Y., Tian, Z.Q., Ma, W., Starks, C.M., *et al.* (2004) Isolation and Characterization of Novel Geldanamycin Analogues. *Journal of Antibiotics*, **57**, 421-428.  
<https://doi.org/10.7164/antibiotics.57.421>
- [19] Jongrungruangchok, S., Tanasupawat, S., Kittakoop, P., Bavovada, R., Kobayashi, H., *et al.* (2006) Identification of *Streptomyces* and *Kitasatospora* Strains from Thai Soils with Geldanamycin Production Strain. *Actinomycetologica*, **20**, 10-14.  
<https://doi.org/10.3209/saj.20.10>
- [20] Taechowisan, T., Chaisaeng, S., Puckdee, W. and Phutdhawong, W.S. (2019) Anti-Inflammatory Activity of Biphenyls from *Streptomyces* sp. BO07 in LPS-Induced RAW 264.7 Cells. *Asian Journal of Biological Sciences*, **12**, 148-155.
- [21] Roe, S., Prodromou, C., O'Brien, R., Ladbury, J., Piper, P., *et al.* (1999) Structural Basis for Inhibition of the Hsp90 Molecular Chaperone by the Antitumor Antibio-

- tics Radicicol and Geldanamycin. *Journal of Medicinal Chemistry*, **42**, 260-266. <https://doi.org/10.1021/jm980403y>
- [22] Ochel, H.J., Eichhorn, K. and Gademann, G. (2001) Geldanamycin, the Prototype of a Class of Antitumor Drugs Targeting the Heat Shock Protein 90 Family of Molecular Chaperones. *Cell Stress Chaperones*, **6**, 105-112. [https://doi.org/10.1379/1466-1268\(2001\)006<0105:GTPOAC>2.0.CO;2](https://doi.org/10.1379/1466-1268(2001)006<0105:GTPOAC>2.0.CO;2)
- [23] Scheufler, C., Brinker, A., Bourenkov, G., Pegoraro, S., Moroder, L., *et al.* (2000) Structure of TPR Domain-Peptide Complexes, Critical Elements in the Assembly of the Hsp70-Hsp90 Multichaperone Machine. *Cell*, **101**, 199-210. [https://doi.org/10.1016/S0092-8674\(00\)80830-2](https://doi.org/10.1016/S0092-8674(00)80830-2)
- [24] Davis, M. and Carbott, D. (1999) Herbimycin A and Geldanamycin Inhibit Okadaic Acid-Induced Apoptosis and p38 Activation in NRK-52E Renal Epithelial Cells. *Toxicology and Applied Pharmacology*, **161**, 59-74. <https://doi.org/10.1006/taap.1999.8765>
- [25] Bijlmakers, M.J. and Marsh, M. (2000) Hsp90 Is Essential for the Synthesis and Subsequent Membrane Association, but Not the Maintenance, of the Src-Kinase p56lck. *Molecular Biology of the Cell*, **11**, 1585-1595. <https://doi.org/10.1091/mbc.11.5.1585>
- [26] Richter, K. and Buchner, J. (2001) Hsp90, Chaperoning Signal Transduction. *Journal of Cellular Physiology*, **188**, 281-290. <https://doi.org/10.1002/jcp.1131>
- [27] Pritchard, K.A., Ackerman, A.W., Gross, E.R., Stepp, D.W., Shi, Y., *et al.* (2001) Heat Shock Protein 90 Mediates the Balance of Nitric Oxide and Superoxide Anion from Endothelial Nitric-Oxide Synthase. *Journal of Biological Chemistry*, **276**, 17621-17624. <https://doi.org/10.1074/jbc.C100084200>
- [28] Schulte, T.W., An, W.G. and Neckers, L.M. (1997) Geldanamycin-Induced Destabilization of Raf-1 Involves the Proteasome. *Biochemical and Biophysical Research Communications*, **239**, 655-659. <https://doi.org/10.1006/bbrc.1997.7527>
- [29] Pratt, W. (1998) The Hsp90-Based Chaperone System, Involvement in Signal Transduction from a Variety of Hormone and Growth Factor Receptors. *Proceedings of the Society for Experimental Biology and Medicine*, **217**, 420-434. <https://doi.org/10.3181/00379727-217-44252>
- [30] Sakagami, M., Morrison, P. and Welch, W. (1999) Benzoquinoid Ansamycins (Herbimycin A and Geldanamycin) Interfere with the Maturation of Growth Factor Receptor Tyrosine Kinases. *Cell Stress Chaperones*, **4**, 19-28. [https://doi.org/10.1379/1466-1268\(1999\)004<0019:BAHAAG>2.3.CO;2](https://doi.org/10.1379/1466-1268(1999)004<0019:BAHAAG>2.3.CO;2)
- [31] Schnaider, T., Somogyi, J., Csermely, P. and Szamel, M. (2000) The Hsp90-Specific Inhibitor Geldanamycin Selectively Disrupts Kinase-Mediated Signaling Events of T-Lymphocyte Activation. *Cell Stress Chaperones*, **5**, 52-61. [https://doi.org/10.1379/1466-1268\(2000\)005<0052:THSIGS>2.0.CO;2](https://doi.org/10.1379/1466-1268(2000)005<0052:THSIGS>2.0.CO;2)
- [32] Whitesell, L. and Cook, P. (1996) Stable and Specific Binding of Heat Shock Protein 90 by Geldanamycin Disrupts Glucocorticoid Receptor Function in Intact Cells. *Molecular Endocrinology*, **10**, 705-712.
- [33] Bamberger, C., Wald, M., Bamberger, A. and Schulte, H. (1997) Inhibition of Mineralocorticoid and Glucocorticoid Receptor Function by the Heat Shock Protein 90-Binding Agent Geldanamycin. *Molecular and Cellular Endocrinology*, **131**, 233-240. [https://doi.org/10.1016/S0303-7207\(97\)00115-9](https://doi.org/10.1016/S0303-7207(97)00115-9)
- [34] Fliss, A., Benzeno, S., Rao, J. and Caplan, A. (2000) Control of Estrogen Receptor Ligand Binding by Hsp90. *Journal of Steroid Biochemistry and Molecular Biology*, **72**, 223-230. [https://doi.org/10.1016/S0960-0760\(00\)00037-6](https://doi.org/10.1016/S0960-0760(00)00037-6)



- [35] Neckers, L., Schulte, T. and Mimnaugh, E. (1999) Geldanamycin as a Potential Anticancer Agent, Its Molecular Target and Biochemical Activity. *Investigational New Drugs*, **17**, 361-373. <https://doi.org/10.1023/A:1006382320697>
- [36] Sugita, T., Tanaka, S., Murakami, T., Miyoshi, H. and Ohnuki, T. (1999) Immuno-Suppressive Effects of the Heat Shock Protein 90-Binding Antibiotic Geldanamycin. *Biochemistry and Molecular Biology International*, **47**, 587-595.
- [37] Bucci, M., Roviezzo, F., Cicala, C., Sessa, W. and Cirino, G. (2000) Geldanamycin: an Inhibitor of Heat Shock Protein 90 (Hsp90) Mediated Signal Transduction Has Anti-Inflammatory Effects and Interacts with Glucocorticoid Receptor *in Vivo*. *British Journal of Pharmacology*, **131**, 13-16. <https://doi.org/10.1038/sj.bjp.0703549>
- [38] Grenert, J., Sullivan, W., Fadden, P., Haystead, T., Clark, J., *et al.* (1997) The Amino-Terminal Domain of Heat Shock Protein 90 (hsp90) That Binds Geldanamycin Is an ATP/ADP Switch Domain That Regulates hsp90 Conformation. *Journal of Biological Chemistry*, **272**, 23843-23850. <https://doi.org/10.1074/jbc.272.38.23843>
- [39] Mandler, R., Wu, C., Sausville, E., Roettinger, A., Newman, D., *et al.* (2000) Immunoconjugates of Geldanamycin and Anti-HER2 Monoclonal Antibodies, Antiproliferative Activity on Human Breast Carcinoma Cell Lines. *Journal of the National Cancer Institute*, **92**, 1573-1581. <https://doi.org/10.1093/jnci/92.19.1573>
- [40] Nimmanapalli, R., O'Bryan, E. and Bhalla, K. (2001) Geldanamycin and Its Analogue 17-Allylamino-17-Demethoxygeldanamycin Lowers Bcr-Abl Levels and Induces Apoptosis and Differentiation of Bcr-Abl-Positive Human Leukemic Blasts. *Cancer Research*, **61**, 1799-1804.
- [41] Yang, J., Yang, J.M., Iannone, M., Shih, W., Lin Y., *et al.* (2001) Disruption of the EF-2 Kinase/Hsp90 Protein Complex: A Possible Mechanism to Inhibit Glioblastoma by Geldanamycin. *Cancer Research*, **61**, 4010-1016.
- [42] Murphy, P., Sharp, A., Shin, J., Gavriluk, V., Dello, C., *et al.* (2002) Suppressive Effects of Ansamycins on Inducible Nitric Oxide Synthase Expression and the Development of Experimental Autoimmune Encephalomyelitis. *Journal of Neuroscience Research*, **67**, 461-470. <https://doi.org/10.1002/jnr.10139>
- [43] Byrd, C., Bornmann, W., Erdjument-Bromage, H., Tempst, P. and Pavle-Tich, N. (1999) Heat Shock Protein 90 mediates Macrophage Activation by Taxol and Bacterial Lipopolysaccharide. *Proceedings of the National Academy of Sciences of the United States of America*, **96**, 5645-5650. <https://doi.org/10.1073/pnas.96.10.5645>
- [44] Zhu, F.G. and Pisetsky, D.S. (2001) Role of the Heat Shock Protein 90 in Immune Response Stimulation by Bacterial DNA and Synthetic Oligonucleotides. *Infection and Immunity*, **69**, 5546-5552. <https://doi.org/10.1128/IAI.69.9.5546-5552.2001>
- [45] Kastelic, T., Schnyder, J., Leutwiler, A., Traber, R., Streit, B., *et al.* (1996) Induction of Rapid IL-1 Beta mRNA Degradation in THP-1 Cells Mediated through the AU-Rich Region in the 3'UTR by a Radicicol Analogue. *Cytokine*, **8**, 751-761. <https://doi.org/10.1006/cyto.1996.0100>
- [46] Wax, S., Piecyk, M., Maritim, B. and Anderson, P. (2003) Geldanamycin Inhibits the Production of Inflammatory Cytokines in activated Macrophages by Reducing the Stability and Translation of Cytokine Transcripts. *Arthritis & Rheumatology*, **48**, 541-550. <https://doi.org/10.1002/art.10780>
- [47] Igarashi, Y., Ohnishi, K., Irie, K. and Murakami, A. (2016) Possible Contribution of Zerumbone-Induced Proteo-Stress to Its Anti-Inflammatory Functions via the Activation of Heat Shock Factor 1. *PLoS ONE*, **11**, e0161282.

<https://doi.org/10.1371/journal.pone.0161282>

- [48] Puri, S.C., Verma, V., Amna, T., Qazi, G.N. and Spiteller, M. (2005) An Endophytic Fungus from *Nothapodytes foetida* That Produces Camptothecin. *Journal of Natural Products*, **68**, 1717-1719. <https://doi.org/10.1021/np0502802>
- [49] Kusari, S., Zühlke, S. and Spiteller, M. (2009) An Endophytic Fungus from *Camptotheca acuminata* That Produces Camptothecin and Analogues. *Journal of Natural Products*, **72**, 2-7. <https://doi.org/10.1021/np800455b>
- [50] Kusari, S., Zühlke, S. and Spiteller, M. (2011) Effect of Artificial Reconstitution of the Interaction between the Plant *Camptotheca acuminata* and the Fungal Endophyte *Fusarium solani* on Camptothecin Biosynthesis. *Journal of Natural Products*, **74**, 764-775. <https://doi.org/10.1021/np1008398>
- [51] Shweta, S., Zuehlke, S., Ramesha, B.T., Priti, V., Kumar, P.M., *et al.* (2010) Endophytic Fungal Strains of *Fusarium solani*, from *Apodytes dimidiata* E. Mey. ex Arn (Lcacinaceae) Produce Camptothecin, 10-Hydroxycamptothecin and 9-Methoxycamptothecin. *Phytochemistry*, **71**, 117-122. <https://doi.org/10.1016/j.phytochem.2009.09.030>
- [52] Jia, M., Chen, L., Xin, H.L., Zheng, C.J., Rahman, K., *et al.* (2016) A Friendly Relationship between Endophytic Fungi and Medicinal Plants: A Systematic Review. *Frontiers in Microbiology*, **7**, 906. <https://doi.org/10.3389/fmicb.2016.00906>
- [53] Al-Tai, A., Kim, B., Kim, S.B., Manfio, G.P. and Goodfellow, M. (1999) *Streptomyces malaysiensis* sp. nov., a New Streptomycete Species with Rugose, Ornamented Spores. *International Journal of Systematic Bacteriology*, **49**, 1395-1402. <https://doi.org/10.1099/00207713-49-4-1395>
- [54] Sazak, A., Şahin, N., Güven, K., Işık, K. and Goodfellow, M. (2011) *Streptomyces samsunensis* sp. nov., a Member of the *Streptomyces violaceusniger* Clade Isolated from the Rhizosphere of *Robinia pseudoacacia*. *International Journal of Systematic Bacteriology*, **61**, 1309-1314. <https://doi.org/10.1099/ijs.0.021329-0>